ACS APPLIED BIO MATERIALS

Article

A Metal–Organic Framework-Enhanced ELISA Platform for Ultrasensitive Detection of PD-L1

Sareh Zhand, Amir Razmjou, Shohreh Azadi, Sajad Razavi Bazaz, Jesus Shrestha, Mahsa Asadnia Fard Jahromi, and MAJID Ebrahimi Warkiani

ACS Appl. Bio Mater., **Just Accepted Manuscript** • DOI: 10.1021/acsabm.0c00227 • Publication Date (Web): 02 Jun 2020

Just Accepted

is published by the American Chemical Society. 1155 Sixteenth Street N.W., Washington, DC 20036

A Metal–Organic Framework-Enhanced ELISA Platform for Ultrasensitive Detection of PD-L1

Sareh Zhand[1], Amir Razmjou[2, 3*], Shohreh Azadi[4], Sajad Razavi Bazaz[1,5], Jesus Shrestha[1], Mahsa Asadnia Fard Jahromi[1,4] Majid Ebrahimi Warkiani[1,5,6*]

[1]School of Biomedical Engineering, University of Technology Sydney, Sydney, New South Wales 2007, Australia

[2]UNESCO Centre for Membrane Science and Technology, School of Chemical Engineering, University of New South Wales, Sydney 2052, Australia

[3]Department of Biotechnology, Faculty of Advanced Sciences and Technologies, University of Isfahan, Isfahan 73441-81746, Iran

[4]School of Engineering, Macquarie University, Sydney, New South Wales 2109, Australia

[5]Institute for Biomedical Materials and Devices, Faculty of Science, University of Technology Sydney, New South Wales 2007, Australia

[6] Institute of Molecular Medicine, Sechenov First Moscow State University, Moscow 119991, Russia

* Contact

Majid Ebrahimi Warkiani (majid.Warkiani@uts.edu.au)

School of Biomedical Engineering, University Technology Sydney, Sydney, New South Wales 2007, Australia

Amir Razmjou (amirr@unsw.edu.au)

UNESCO Centre for Membrane Science and Technology, School of Chemical Engineering, University of New South Wales, Sydney 2052, Australia

Abstract:

The programmed cell death ligand 1 (PD-L1) protein has emerged as a predictive cancer biomarker for sensitivity to immune checkpoint blockade-based cancer immunotherapies. Current technologies for the detection of protein-based biomarkers, including the enzyme-linked immunosorbent assay (ELISA), have limitations such as low sensitivity and limit of detection (LOD) and in addition to degradation of antibodies in exposure to environmental changes such as temperature and pH. To address these issues, we have proposed a metal-organic framework (MOF)-based ELISA for the detection of the PD-L1. A protective coating based on Zeolitic Imidazolate Framework 8 (ZIF-8) MOF thin film and polydopamine-polyethyleneimine (PDA-PEI) was introduced on an ELISA plate for the improvement of antibody immobilization. Sensitivity and LOD of the resulting platform was compared with a conventional ELISA kit, and the bioactivity of the antibody in the proposed immunoassay was investigated in response to various pH and temperature. The LOD and sensitivity of the MOF-based PD-L1 ELISA was 225 and 15.12 times higher, respectively, compared with that of the commercial ELISA kit. The antibody@ZIF-8/PDA-PEI was stable up to 55°C and a pH range of 5-10. The proposed platform can provide sensitive detection for target proteins, in addition to be resistant to elevated temperature and pH. The proposed MOF-based ELISA has significant potential for the clinical and diagnostic studies.

Keywords: Metal-Organic Framework; ZIF-8; PD-L1; Enzyme-linked immunosorbent assay; Limit of Detection.

Introduction

In the past decades, the socioeconomics burden of diseases, including cancer, has rapidly increased. To reduce this burden, fast and accurate diagnosis plays an important role in early detection and hence the treatment of diseases. Therefore, the demand for novel diagnostic technologies that benefit from high specificity and sensitivity to accompany clinical diagnosis has been increased.[1] One of the most straightforward approaches for screening cancer patients is the detection and measurement of protein biomarker levels in biological samples, e.g., blood. Owing to the complexity and heterogeneity of cancer, rapid and accurate measurement of protein biomarkers is a challenging issue that requires further investigation.[2]

The programmed cell death-1/programmed cell death ligand-1 (PD-1/PD-L1) signaling pathway has been shown to play a crucial role in tumor immune invasion.[3] The PD-1 protein is a checkpoint co-inhibitory receptor expressed on the surface of immune cells. Under normal circumstances, PD-1 causes a negative feedback mechanism that leads to switching off the activation of T cells. This phenomenon prevents tissue-damaging during stimulation of the immune system.[4] The PD-L1 protein on the surface of tumor cells (or antigen-presenting cells, dendritic cells, and macrophages) could directly bind to PD-1. This process limits the activation and proliferation of T cells and weakens their cytotoxicity against tumor cells.[5, 6] This mechanism is known for tumor immune escape,[5, 6] which makes the expression level of PD-L1 an important immune checkpoint.[7]

The detection of PD-L1 and the measurement of its expression level have demonstrated significant potential for monitoring cancer progression and response to immunotherapy. Current immunoassay technologies for the cancer biomarker detection, including the enzyme-linked immunosorbent assay (ELISA) are accurate and simple.[8] Despite the current progress in the development of immunosensors, microfluidic and point-of-care technologies, ELISA has been

identified as a gold standard and is the most widely used immunoassay technique for detecting and measuring disease biomarkers.[9] However, there are some inevitable limitations in the use of ELISA, including limited sensitivity,[10] which requires novel strategies to improve the ELISA limit of detection (LOD) and the need for reagents with high specific affinity, such as monoclonal antibodies (mAbs), that are not only expensive but also suffer from quality variations during production.[11] Moreover, antibodies can degrade owing to temperature changes, corrosion from chemical reagents, and other perturbation conditions, which consequently affects the efficiency of the immunoassay.[12] Therefore, stringent storage conditions (e.g., refrigeration at 4°C) are usually required to maintain their stability.

Several strategies have been developed to improve the performance of traditional ELISA[13]. Nanotechnology has provided a significant number of solutions. The most common strategies that are currently used to functionalize antibodies onto nanoparticles are covalent immobilization or direct physical adsorption .[14]

During the last three decades, a wide range of antibody (Ab) immobilization chemistries have been developed through novel lab-on-a-chip technologies and biosensors, which has enhanced the performance of immunoassays.[15] The performance of an immunoassay critically depends on the characteristics of the immobilized Ab because the detection sensitivity, reproducibility, robustness, and other bioanalytical parameters depend on the immobilization step. Therefore, the development of suitable strategy for immobilization of antibodyis a critical requirement that would affect the analytical performance of an immunoassay significantly.[16]

Various antibody immobilization methods have been employed for the preparation of immunoassays, including covalent/noncovalent bonding, oriented, site-specific, peptide nucleic acid (PNA)- as well as DNA-directed, and recombinant antibody binding.[16] However, the

immobilization of antibodies limits their movement, which could affect their three-dimensional conformation. These immobilization techniques suffer from critical limitations including random antibody orientation, nonspecific binding, low stability, uncontrolled immobilized-antibody density, antibody denaturation and conformation change, reduced antibody functional activity, and the need for extra reagents including cross-linkers, fragment crystallizable (Fc)-binding proteins, custom manufactured recombinant antibodies, and bioconjugate DNA/PNA.16

A metal–organic framework (MOF) is a kind of hybrid material containing metal ions or clusters coordinated to organic linkers. It possesses a large surface area, high porosity in addition to a tunable pore size.[17] These features make MOFs suitable candidates in various applications including catalysis,[18] gas storage,[19] sensors,[20] and functional devices.[21] MOFs as a tool for the encapsulation of biomolecules has been a matter of research studies in recent years.[22, 23] It has been shown that enzymes encapsulated in a MOF show limited structural changes, leading to maintenance of the biological function of the enzyme even under denaturing conditions.[24] Naik and co-workers investigated the effect of MOF coatings on the preservation of the biorecognition capability of bio-conjugated antibodies after exposure to high temperatures (40°C and 60°C). They found that the stability of antibodies was improved in a wide temperature range, which might be practical for the fabrication of antibody-based biochips.[25] The porous structure of MOFs could potentially protect the biomolecules from environmental conditions and improve their activity. MOFs-based biomineralization has been used for the transport, storage, sensing, and treatment of cargos including biomolecules, biological catalysts, and living organisms.[26]

Despite the many available strategies for ELISA fabrication, for the first time, we have introduced the application of MOFs for the fabrication of an ELISA platform. MOFs have possessed nanoporous system with thermal stability and tunable physicochemical properties.

Furthermore, MOFs can be introduced as a host for encapsulation of biomolecules due to their ability to protect the biomolecules from rigorous environments and protect their biological functions [27]. Moreover, due to a unique composition, diverse structures, and tunable size MOFs are an excellent alternative for novel immunoassay [28]. The MOF-based polymeric nanoparticles provide the large surface-to-volume ratios which promote the efficient immobilization of antibodies on the nanoscale surface that consequently increase the capture efficiency of substrate surfaces.

Herein, a new strategy for the immobilization of antibodies on an ELISA plate using MOFs to form an antibody@MOF composite is presented. Pretreatment of the surface of the plate with a binding agent is critical to obtain an antibody@MOF layer that is more stable and possess high integrity. Therefore, the polystyrene pattern coated with polydopamine-polyethyleneimine (PDA-PEI) was utilized to induce the basement for the nucleation of the antibody@MOF composite on a polystyrene substrate. PEI contains abundant NH_2 groups to covalently immobilize PD-L1 antibodies. The Zeolite Imidazolate Framework-8 (ZIF-8) MOF was selected based on the following features: (a) biocompatibility and biodegradability (low cytotoxicity); (b) low cost and long durability,[29, 30] and (c) high stability under experimental conditions (e.g., higher temperatures and extremely alkaline and acidic conditions) that are harsher than those used for ELISA.[31, 32] In this article, we describe a simple method based on ELISA method for the development of an inexpensive, rapid and highly-sensitive *in vitro* diagnostics kit. This proposed immobilization approach only encompasses the addition of an antibody to ZIF-8 to form a stable complex on the PDA-PEI pattern on the polystyrene surface. The fabricated MOF-based ELISA improved the LOD and stability of the conventional ELISA kit under perturbation conditions, which demonstrated its potential to significantly improve current immunoassays.

Experimental section

Materials

A microtitre ELISA plate was purchased from FALCON (U.S.A), Human PD-L1 Simple Step ELISA® Kit was provided by Abcam (Cat No ab214565, Australia), Tris (hydroxylmethyl) aminomethane, dopamine hydrochloride (DA), polyethyleneimine (PEI, Mw=1000 Da), 2-methylimidazole, phosphate buffered saline (PBS) and zinc nitrate hexahydrate were purchased from Sigma–Aldrich (USA).

Polydopamine coating of polystyrene microtiter ELISA plates

A polystyrene microtiter ELISA plate was coated with a thin layer of PDA-PEI based on a previously published protocol.[33] A PDA film can form on organic/inorganic surfaces through self-polymerization of dopamine under alkaline conditions.[34] PEI in the dual polymerization of PDA-PEI, endures Michael addition or Schiff-base reactions with a catechol group in PDA to produce a strong bio-adhesive layer on the surface of substrate. Therefore, the role of PEI was as a cross-linking agent with PDA. [35] Briefly, each well of a microtiter ELISA plate as the model substrate was treated with 200 µL of freshly prepared solution of dopamine hydrochloride (2 mg/mL), PEI (1000 MW, 2 mg/mL) in Tris-buffer solution (0.05 M, pH 8.5). The treated plate was incubated overnight at room temperature and washed three times with Milli-Q® water. For each experiment, a fresh dopamine hydrochloride solution was used to prevent premature polymerization of dopamine.

Preparation of antibody@ZIF-8

ZIF-8 was used as a representative MOF structure in this study. ZIF-8 was synthesized through a self-assembly process, as previously described [33]. Briefly, the ZIF-8 precursor solution was prepared from zinc nitrate hexahydrate, $Zn(NO_3)_2 \cdot 6H_2O$ (0.027 g) and 2-methyl imidazole, (0.566 g) in a total volume of 10 mL Milli-Q® water. Both the detector and capture anti-PD-L1

antibodies (from Abcam ELISA kit) were provided in 10× concentration and mixed with a ZIF-8 solution to obtain a 1× concentration, dispensed into the PDA-PEI coated wells, and incubated for 60 min at room temperature using a plate shaker. A schematic illustration of the workflow is shown in Figure 1. The resultant antibody@ZIF-8/PDA-PEI was used for a highly sensitive immunoassay of PD-L1.

Surface characterization

The structure of the antibody@ZIF-8/PDA-PEI was characterized by using microscopy imaging and spectroscopic techniques. Scanning electron microscopy (SEM) was used to probe the surface morphology of the modified microtiter ELISA plate. The modified surfaces were sputter-coated with a 15 nm Au/Pd coating under vacuum to achieve a good conductivity. SEM images were then taken using a scanning electron microscope (ZEISS SUPRA55VP, USA) with an accelerating voltage of 5 keV. The thickness of the ZIF-8 and PDA-PEI on the surface of the microtiter ELISA plate was measured by atomic force microscopy (AFM; Park systems XE7). A V-shaped cantilever with a frequency of 286.2 kHz was used to capture the surface morphology in nonconductive mode. The average values of the roughness were reported to determine the surface roughness of the polymer films on a scan area of 5.0 μm × 5.0 μm. The captured topographical images were analyzed using ProfilmOnline and Gwyddion 2.55 software.

The chemical composition of the modified microtiter ELISA plate wells was analyzed by Fourier-transform infrared spectroscopy (FT-IR) (MIRacle 10, Shimadzu, USA). FT-IR spectra were acquired in triplicate in the range of 4000–400 cm^{-1} with a resolution of 4 cm^{-1} and averaging 16 scans for each spectrum. Furthermore, powder X-ray diffraction (XRD) (D8 Discover BRUKER) was performed to identify the ZIF-8 crystalline structure on the surface of the PDA-PEI-coated microtiter ELISA plate. Crystallographic data of the antibody@ZIF-8/PDA-PEI patterns was obtained by scanning the sample through a 2θ range of 5–40^{o} with a step size of

0.019° and 1 second per step. The XRD data analysis was performed using High Score Plus software and compared with the database from the International Center for Diffraction Data.

The water contact angle (WCA) was measured using a drop shape analyzer (DSA 100, Kruss, Germany) and One Attension software (14 μL, a geometrical method sessile drop, water, formamide, and glycerol). An image of a water droplet on the surface of a microtiter ELISA plate, PDA-PEI -coated, and PDA-PEI /ZIF-8-coated surface was captured with a CCD camera. The contact angles were calculated by drawing a tangent line near the edge of each droplet; the values are reported as the average of three measurements performed at three locations on the surface. Additionally, to probe the intermolecular interactions at the interface surface free energy (SFE) of a solid was calculated using the Oss and Good acid-base method from the contact angle measurement.[36]

Detection of PD-L1 using the modified ELISA

The detection of the PD-L1 antigen was performed using three different platforms including the commercial ELISA kit, modified ELISA in PDA-PEI -coated wells, and modified ELISA using antibody@ZIF-8/PDA-PEI. To achieve standard curves, which were defined as the optical density (OD) versus the protein concentration, eight concentrations of PD-L1 (0, 21.88, 43.75, 87.5, 175, 350, 700, and 1400 pg/mL) were prepared and examined using the three configurations based on the ELISA protocol. Briefly, the precursors of ZIF-8 were added to the microtiter ELISA plate wells coated with PDA-PEI and incubated with both capture and detector antibodies for 60 minutes at room temperature. Then, the wells were washed with the washing buffer and incubated with 3,3',5,5'-tetramethylbenzidine (TMB) development solution for 10 min. Finally, the stop solution was added and the OD was immediately recorded at 450 nm. For statistical analysis , the OD measurements were conducted in triplicate. A concentration of 0

pg/mL of PD-L1 antigen, which means, no addition of antigen, was used to examine whether the PDA-PEI and ZIF-8/PDA-PEI platforms show self-absorbance in the immunoassay.

Examining the stability of antibody@ZIF-8 at various pH and temperatures

We hypothesized that MOF can be a powerful class of material for preserving the stability of antibodies at various temperatures and pH. To test this hypothesis, the activity of the antibodies in both antibody@ZIF-8/PDA-PEI ELISA and commercial ELISA was assessed under different pH and temperature conditions. The antibody@ZIF-8 was incubated for 10 min at room temperature to form the ZIF-8 crystals around the antibody. The resulting antibody@ZIF-8 composite and the original antibody as a control were placed in microtubes and subjected to various temperatures ranging from 45°C to 85°C at 10°C intervals for 30 min. Then, the PD-L1 antigen at a concentration of 350 pg/mL was added to each mixture, moved to the microtiter ELISA plate well, and incubated for 60 min at room temperature. After incubating with TMB and a stop solution, the OD was recorded at 450 nm.

In order to examine the stability of the antibody@ZIF-8 at various pH, PBS solution with different pH values (ranging from 5 to 10 with an increment of 1) were used. Both the capture and detector antibody@ZIF-8 mixture was incubated with PD-L1 antigen at a concentration of 350 pg/mL. The PBS solution with different pH were added to wells and allowed to stand for 60 min, whereas in the control group, both the capture and detector antibodies without ZIF-8 were subjected to various pH treatments.

The sensitivity measurements

To assess the sensitivity of the MOF-based ELISA, the concentration of the capture and detector antibodies was further decreased 20, 100, and 200 times, which we named 0.05x, 0.01x, and 0.005x, and a PD-L1 ELISA was conducted in three different types of wells, (conventional

ELISA, PDA-PEI -coated, and antibody@ZIF-8/PDA-PEI). The LOD was calculated according to the standard formula reported in the literature.[37, 38]

The Sensitivity was calculated by measuring the slope of ELISA standard curve (Absorbance / concentration of antibody (absorbance/pg/mL)).

Statistical analysis:

Statistical analysis of ELISA in all three studied platforms including: antibody@ZIF-8/PDA-PEI, conventional ELISA in PDA-PEI coated wells and conventional ELISA in exposure to elevated temperatures and various pH was performed using T-test in SPSS 22 software. Experiments were carried out at least three times. Statistically significances was measured as the $p < 0.05$.

Results and discussions

Surface characterization

SEM images showed the morphologies of polystyrene substrate with and without ZIF-8 precursors are quite distinctive and the PDA-PEI coating formed a dense, thick film above the polystyrene microtiter ELISA wells (Figure 2A). The antibody@ZIF-8 platform had the same polyhedral morphology as pristine ZIF-8 (Figure 2AI, II) the small size of antibody protein makes them invisible at this magnification. Due to the presence of a wide range of functional groups in proteins (such as carbonyl, hydroxyl ,carboxyl, and imidazole groups), they consider as nucleation sites for the formation of ZIF-8 crystals.[39] Besides, SEM images illustrate that the crystal morphology of ZIF-8 uniquely depended on the antibody. These images indicated that the microtiter ELISA wells were successfully covered by a hydrophilic PDA-PEI layer.

The AFM image of the microtiter ELISA well in Figure 2B IV showed the native microtiter ELISA well is a flat surface. In comparison, the image displayed in Figure 2B III demonstrated that a nano-sized thin film was distributed on the surface uniformly with enhanced roughness

after treatment with ZIF-8. Based on Figure 2BII numerous evenly distributed sharp peaks on the microtiter ELISA well surface that previously coated with PDA-PEI confirmed the ZIF-8 formation on the surface. The average values of the roughness of all surfaces were measured by atomic force microscopy That sensed the surface roughness of the sampleby a change in the laser beam and the deflection of the cantilever,[40]; thus it can generate the topography of surface. The results were analyzed using Gwyddion 2.55 software, which indicated average roughness values of 20.47 nm, 13.22 nm, 5.296 nm, and 180 pm for the antibody@ZIF-8/PDA-PEI, ZIF-8/PDA-PEI, PDA-PEI, and empty microtiter ELISA wells, respectively.

In Figure 2BI the distribution of multiple sharp peaks on the PDA-PEI treated microtiter ELISA well surface demonstrated the morphology of antibody@ZIF-8-loaded PDA-PEI treated surface. Overall, the observations made from the SEM and AFM images confirmed that both PDA-PEI and ZIF-8 could increase the surface roughness and consequently prepare larger surface area for PD-L1 antibodies to be immobilized on the ZIF-8/PDA-PEI-derived microtiter ELISA well surface, which is suitable for the formation of a sandwich-type ELISA format.

The functional groups present in the structures of PDA-PEI and ZIF-8 were identified using FT-IR (Figure 3A). Strong bands at 3135, 2929, 1635, 1585, 1510, 1367, 1333, 1146 and 426 cm^{-1} were observed in the FT-IR spectrum of the ZIF-8 sample after formation of ZIF-8 on the PDA-PEI patterning. The peaks detected at 3135 and 2929 cm^{-1} were attributed to aromatic and aliphatic C–H asymmetric stretching vibrations, respectively. The signal at approximately 1635 cm^{-1} was attributed to the C=C stretching mode, whereas the band at 1585 cm^{-1} corresponded to the C=N stretch vibration. The peaks at 1300–1460 cm^{-1} and 1146 cm^{-1}were attributed to the entire aromatic ring stretching, and aromatic C–N stretching mode, respectively. Interestingly, a sharp Zn–N stretching vibration band was observed at 426 cm^{-1}, which suggested the formation

of an imidazolate through the chemical combination of zinc ions and nitrogen atoms of the methyl imidazole groups.[41] The FT-IR spectrum of the surface modified with PDA-PEI patterning contained a peak in the 1510–1560cm^{-1} range, which was attributed to N–H vibrations, and a peak between 3200–3400 cm^{-1}, which indicated the presence of hydroxyl groups. The FT-IR spectrum of the antibodies@ZIF-8 contained stretches at 1530 cm^{-1} owing to the presence of antibodies, which corresponded with the characteristic amide II band (mainly from a combination of NH bending and CN stretching modes). Furthermore, in the FT-IR spectrum of antibodies@ZIF-8/PDA-PEI, shifting the amide vibrational mode for the antibodies to a higher wave number indicated strong interactions between the antibody and the ZIF-8 due to the coordination between the Zn cations and the carbonyl group of the protein. The characteristic ZIF-8 peak at 426 cm^{-1} was also observed in the antibodies@ZIF-8/PDA-PEI, confirming the formation of a ZIF-8 structure. The FT-IR results for ZIF-8 and antibody@ZIF-8 were consistent with the results of Feng *et al.*, showing the presence of the same functional group.[42] Moreover, Mohammad and co-workers reported similar FT-IR peaks for PDA-PEI patterning.[33]

The XRD pattern of ZIF-8/PDA-PEI consisted of a broad peak owing to the presence of amorphous PDA-PEI. The XRD pattern was consistent with the dominant sharp peaks displayed by simulated ZIF-8 patterns;[43] additionally for antibody@ZIF-8/PDA-PEI, the discrete peaks recognized were at 2θ of 18.02° , 12.7°, 10.3° and 7.3°, corresponding to 222, 211, 200 and 110, orientations, respectively (Figure 3B). These results prove the existence of crystal structure of ZIF-8.

Changing the surface chemistry and microstructure could tuned the wetting properties of a surface The calculated WCAs and the corresponding SFEs of the modified surfaces are shown in Figure 3C. The WCA of polystyrene significantly reduced from 65.77° to 54.23° after the PDA-

PEI patterning, whereas the SFE increased from 47.2 mN/m to 61.7 mN/m. We attributed these changes to the changes in the surface chemistry owing to the higher number of the catechol group, which increased the surface chemical attraction to molecules of water and enhanced the hydrophilicity. The increase in the hydrophilicity after the introduction of the PDA-PEI coating was due to the chemical nature of the PDA layer. Mohammad *et al.*[33] also reported enhancement of the hydrophilicity after coating an ELISA plate with PDA-PEI. It has been shown that an increase in roughness results in increasing hydrophilicity.[44] Our results demonstrated that the formation of ZIF-8 and antibody@ZIF-8/PDA-PEI thin films slightly decreased the WCA from 65.77° in polystyrene to 25.14° and 30.48° in ZIF-8 and antibody@ZIF-8/PDA respectively. The change in WCA that make the patterning much more hydrophilic was owing to the ZIF-8 layer formation, which increased the surface rugosity. Wenzel explained the effect of morphology and surface chemistry on the WCA using the following equation (Eq. 1).[45]

$$\text{Cos } \theta = r \text{ Cos } \theta^e \quad (1)$$

in which θ^e is the WCA on a flat surface, θ is the apparent contact angle, and r is the ratio of the actual solid/liquid contact area to its vertical projection. An increase in roughness enhances the value of r and results in hydrophilicity. The hydrophilicity resulting from the PDA and ZIF-8 coating led to better absorption of droplets (e.g., antibody) to the surface.[44]

High thermal and pH stability of antibody@ZIF-8

The bio-mineralization of ZIF-8 was owing to the enrichment of precursors on the PDA-PEI-coated wells, which possesses hydrophilicity properties, followed by the chelation of the zinc ion precursors on the surface with the catechol moiety in PDA.[46] This enabled the spontaneous ZIF-8 growth above the PDA-PEI coating.[47-49] The ability of MOFs to preserve the stability of proteins and antibodies is attributed to the tight encapsulation of proteins, which resulted from the small

pore size of the MOF and the coordination interactions between the Zn cations of ZIF-8 and the carbonyl groups of the protein backbone .[39] The loading of biomacromolecules in the pore networks of MOFs could potentially protect them from the outer environment. Moreover, it has been demonstrated that the MOF pore structure not only maintains the activity of stored biomolecules but also improves their activity through the self-assembly (biomineralization) process.[26] The results indicated that after heating treatments, the unprotected antibody lost its main activity in ELISA whereas antibody@ZIF-8 maintained its biological activity up to 55°C (Figure 4A). The activity of the antibody@ZIF-8 decreased when the temperature was increased to 65°C. However, the antibody@ZIF-8 structure still showed a higher OD at 65°C compared with the standard ELISA either in empty wells or PDA-PEI -coated wells. The effect of the PDA-PEI coating on the protein stability at various temperatures was much lower than ZIF-8/PDA-PEI; however, its detected OD was still higher than that in commercial ELISA wells. Results of ELISA using antibody@ZIF-8/PDA revealed that by increasing the temperature, the detected OD using the antibody@ZIF-8/PDA platform ELISA will be decreased. However, this reduction compares to that of PDA-PEI coated well ELISA and conventional ELISA was not significant (p value=0.22). To explain quantitatively, the detected OD in conventional ELISA in exposure to elevated temperature (45ºC) showed a dramatic decrease from 0.8 to 0.2, and by increasing the temperature to 55ºC, it decreased to 0.17, which is the confirmation for the loss of antibody bioactivity. Similarly, in ELISA performed on PDA-PEI coated wells, detected OD in exposure to elevated temperature (45ºC) showed a sharp decrease from 2 to 0.3, and by increasing the temperature to 55ºC, it decreased to 0.2, which is the confirmation of the loss of antibody bioactivity. However, in antibody@ZIF-8/PDA-PEI platform ELISA the detected OD in exposure to elevated temperature (45ºC) showed a slight decrease from 2.55 to 2.4. By

increasing the temperature to 55ºC, it decreased to 2, which is confirmation of the antibody stability in elevated temperature. However, when the temperature increased to 65ºC, the OD was decreased dramatically to 0.2, which proves the loss of antibody bioactivity (Figure 4A). Similarly, the results clearly proved the stable behavior of antibody@ZIF-8 when exposed to various pH from 5 to 10. The ability of the PDA-PEI coating to maintain the antibody activity at various pH was much lower than ZIF-8; nonetheless, its activity was still higher than the activity of antibodies in commercial ELISA wells (Figure 4B). To explain quantitatively, the detected OD in conventional ELISA in exposure to pH=5 showed a dramatic decrease from 0.8 to 0.15, and by increasing the pH to 10, the OD decreased to 0.07, which proves the antibody lost its bioactivity. Moreover, in ELISA performed using antibody@ZIF-8/PDA-PEI platform, the detected OD in exposure to pH=5 showed a slight decrease from 2.55 to 2.04, and by increasing the pH to 10, the OD decreased to 1.1 that is confirmation of the antibody stability in acidic and alkaline condition (Figure 4B). The reduction of the OD in the antibody@ZIF-8/PDA ELISA, in exposure to various pH compare to that of PDA-PEI coated wells ELISA and conventional ELISA was not significant (p value=0.14). Feng *et al.*[42] showed that protecting antibodies with ZIF-8, ZIF90, and ZIF8X resulted in extraordinary thermal, chemical, and mechanical stabilities. The results in our study indicate that ZIF-8 is a protective agent for biological molecules, which was consistent with the results reported by Feng *et al*. Furthermore, the novel use of MOF for biomineralization of an antibody improved the LOD in an ELISA assay. Tan and co-workers[50] demonstrated similar results by replacing the antibody-conjugated enzymes in ELISA with antibody-covered $Cu_3(PO_4)_2$@PDA nanosheets. They revealed that a high number of attached antibodies to the flat nanosheets resulted in a low detection limit. They also proved the antibody-covered $Cu_3(PO_4)_2$@PDA nanosheets were stable under conditions that are usually not favorable

to enzymatic activity. In another report, Mohammad *et al.*[33] employed a mussel-inspired PDA-PEI coating to pattern horseradish peroxidase (HRP) and glucose oxidase (GOx)-ZIF-8 in microfluidic channels. Their results indicated that *in situ* ZIF-8/GOx&HRP composites prepared on PDA-PEI patterns showed a higher acidic and thermal stability compared to the samples without ZIF-8. More recently, Zhang and co-workers[51] developed a MOF delivery system through the encapsulation of CpG oligodeoxynucleotides (ODNs) into ZIF-8 nanoparticles. Their results emphasize the high stability of ZIF-8/CpG ODNs complexes in various physiological environments. Furthermore, Wang *et al.*[52] were able to maintain the biorecognition capabilities of antibodies exposed to increased temperatures (40 and 60°C) by using MOF coatings of antibodies (IgG/anti-IgG) to immobilize them on sensor surfaces. In the present study, we successfully immobilized antibodies on the surface of microtitre ELISA plates using a simple one-step cost-effective material to improve the LOD of conventional ELISA kit by 225 times and examined their stability at elevated temperatures and a wide pH range to confirm their heat, acidic, and alkaline stability. The configuration used in this work eliminates the need for strict storage conditions for antibodies and preserves the biofunctionality of antibodies in harsh environmental conditions. In another study, Liao and co-workers[24] integrated catalase (CAT) enzyme in ZIF-90 and ZIF-8 microcrystals and showed the enzyme maintained its biological features in a broader variety of conditions, including high temperatures (i.e., 80°C) and addition of denaturing reagent (i.e., urea).

Antibody@ZIF-8 improved LOD and sensitivity of ELISA

We anticipated that the present PDA-PEI - and antibody@ZIF-8/PDA-PEI -coating method would improve the LOD of the immunoassay. The LOD on the PDA-PEI -coated wells (0.313 pg/mL) and antibody@ZIF-8/PDA-PEI -coated wells (0.035 pg/mL) improved 25 times and 225

times, respectively, compared with that of the commercial ELISA kit (7.89 pg/mL). Liu *et al*.[53] used a MOF-based sandwich ELISA system for the detection of alpha-fetoprotein (AFP), a biomarker for liver cancer, however they modified their wells using PEI which could detect 0.02 ng/mL AFP in blood. In the present study the further modification on PDA-PEI coated surface with ZIF-8 leads to thousand time improvement in the LOD compare with their study. Our proposed coating methods improved the detection limit of the PD-L1 immunoassay 25 times, which is much higher than that recently reported by Wang *et al*..[54] They integrated the rabbit anti-mouse immunoglobulin G antibody (RIgG) with Cu-MOF with peroxidase-like activity (RIgG@Cu-MOF) for colorimetric immunoassay detection of mouse IgG (mIgG) in serum. The limit of detection of RIgG@Cu-MOF toward mIgG was 0.34 ng/mL which was 3 times more sensitive than that of horseradish-peroxidase-labeled RIgG. Additionally, they reported a similar stability against pH, high temperature, and long-time storage, using different types of MOFs.

The sensitivity of the antibody@ZIF-8/PDA-PEI ELISA was also studied. The sensitivity of antibody@ZIF-8/PDA-PEI was measured as the value of absorbance over the antibody concentration [33, 55]. The sensitivity of antibody@ZIF-8/PDA-PEI was linear when examined in a low concentration antibody (ranging from 0, 21.88, 43.75, 87.5, and 175 to 350 pg/mL). The ELISA performed using the antibody@ZIF-8/PDA-PEI platform had a higher sensitivity of 0.0862 absorbance/pg/mL compared with the ELISA performed in wells coated with PDA-PEI (0.0424 absorbance/pg/mL) and conventional ELISA (0.005 absorbance/pg/mL; Figure 4D). This indicated 15.12 and 7.4 times higher sensitivity of the antibody@ZIF-8/PDA-PEI and PDA-PEI platforms, respectively, compared with conventional ELISA. Our platform also showed (Figure 4C) that even after decreasing the number of antibodies 200 times; we were still able to obtain the same efficient results as the standard antibody used for ELISA. This makes this

technology more versatile and cost-effective for ELISA and other techniques that use protein and antibody immobilization for biomarker detection. Results of this study showed higher improvement in LOD (225- fold) compare to other published MOF-based ELISA methods[54, 56, 57]. The MOF-based ELISA techniques and other metal and metal oxide-based techniques to improve the LOD of conventional ELISA have been listed in Table 1 and elsewhere[13].

The ELISA results of three different well configurations, commercial ELISA wells, PDA-PEI -coated wells, and PDA-PEI /ZIF-8 coated wells, indicated that the OD in antibody@ZIF-8 wells was higher than that in the PDA-PEI -coated wells, and much higher than that in commercial ELISA wells. These results proved our hypothesis that the ZIF-8/PDA-PEI configuration increased the sensitivity of the immunoassay (Figure 4C). Moreover, both configurations including the PDA-PEI -coated and ZIF-8/PDA-PEI -coated wells did not show any measurable OD in the absence of the PD-L1 antigen, which confirmed that there was not any false-positive absorbance.

We proposed a protective coating approach based on MOFs to proficiently improve the LOD of current ELISAs and also protect antibodies against perturbation environments. To the best of our knowledge, this is the first time that a MOF coating has been used to improve the LOD of a commercial ELISA kit. There are three major factors that could contribute to the enhancement of the LOD and sensitivity of the antibody@MOF in a commercial ELISA kit: 1) The antibody could adsorb physically to the polystyrene surface by interacting with the hydrophobic groups exist in antibody molecules without requirements for ZIF-8/PDA-PEI. A higher Ab immobilization density could be reached on this platform to promote improved the physical adsorption of the antibody onto the polystyrene surface because of the increase in surface roughness, which provides a larger surface area. The higher surface area results in higher

absorption and detection. 2) This platform not only provides the specific orientation for immobilized antibodies owing to the reduction of steric hindrance and tight confinement of the antibodies, but it also inhibits the random and upside down orientation of the antibody, which increases the exposure of the antibody's antigen binding fragment to a higher amount of antigens. 3) The hydrophilicity of the surface is improved as a result of coating with PDA-PEI, which would be beneficial for capturing of antibodies.

Conclusions

A MOF-based sandwich immunoassay was developed for highly sensitive detection of human PD-L1 antigen using modified ELISA. The antibody@MOF was highly stable against elevated temperature and pH, as indicated by no decrease in the detection response when it was exposed to a pH range of 5-10 and a temperature up to 55°C. The proposed method resulted in an LOD of 0.035 pg/mL and 0.313 pg/mL in antibody@ZIF-8/PDA-PEI and PDA-PEI -coated configurations, which was 225 and 25 times more sensitive than conventional ELISA, respectively. The developed immunoassay had a 15.12-fold higher sensitivity compared with the commercially available ELISA, which represent significant potential for the future development of *in vitro* diagnostic kits and immunoassays that are highly sensitive for various disease biomarkers and analytes.

Acknowledgment

The authors would like to warmly thank the Australian Research Council for the support of this project through Discovery Project Grants (DP170103704 and DP180103003) as well as the National Health and Medical Research Council for the Career Development Fellowship

(APP1143377). Some parts of this project were performed at the South Australian node of the Australian National Fabrication Facility under the National Collaborative Research Infrastructure Strategy.

References

1. Hanash, S. M.; Baik, C. S.; Kallioniemi, O., Emerging molecular biomarkers—blood-based strategies to detect and monitor cancer. *Nature reviews Clinical oncology* **2011,** *8* (3), 142.
2. Giljohann, D. A.; Mirkin, C. A., Drivers of biodiagnostic development. *Nature* **2009,** *462* (7272), 461.
3. Azadi, S.; Es, H. A.; Bazaz, S. R.; Thiery, J. P.; Asadnia, M.; Warkiani, M. E., Upregulation of PD-L1 expression in breast cancer cells through the formation of 3D multicellular cancer aggregates under different chemical and mechanical conditions. *Biochimica et Biophysica Acta (BBA)-Molecular Cell Research* **2019,** *1866* (12), 118526.
4. Pardoll, D. M., The blockade of immune checkpoints in cancer immunotherapy. *Nature Reviews Cancer* **2012,** *12* (4), 252.
5. Chen, D. S.; Mellman, I., Elements of cancer immunity and the cancer–immune set point. *Nature* **2017,** *541* (7637), 321.
6. Gibney, G. T.; Weiner, L. M.; Atkins, M. B., Predictive biomarkers for checkpoint inhibitor-based immunotherapy. *The Lancet Oncology* **2016,** *17* (12), e542-e551.
7. Zou, W.; Wolchok, J. D.; Chen, L., PD-L1 (B7-H1) and PD-1 pathway blockade for cancer therapy: Mechanisms, response biomarkers, and combinations. *Science translational medicine* **2016,** *8* (328), 328rv4-328rv4.
8. Bojorge Ramírez, N.; Salgado, A.; Valdman, B., The evolution and developments of immunosensors for health and environmental monitoring: problems and perspectives. *Brazilian journal of chemical engineering* **2009,** *26* (2), 227-249.
9. Vashist, S. K.; Schneider, E. M.; Lam, E.; Hrapovic, S.; Luong, J. H., One-step antibody immobilization-based rapid and highly-sensitive sandwich ELISA procedure for potential in vitro diagnostics. *Scientific reports* **2014,** *4*, 4407.
10. Billingsley, M. M.; Riley, R. S.; Day, E. S., Antibody-nanoparticle conjugates to enhance the sensitivity of ELISA-based detection methods. *PloS one* **2017,** *12* (5), e0177592.
11. Marx, V., Finding the right antibody for the job. Nature Publishing Group 10, 703–707 (2013).
12. Braun, A.; Kwee, L.; Labow, M. A.; Alsenz, J., Protein aggregates seem to play a key role among the parameters influencing the antigenicity of interferon alpha (IFN-α) in normal and transgenic mice. *Pharmaceutical research* **1997,** *14* (10), 1472-1478.
13. Gao, Y.; Zhou, Y.; Chandrawati, R., Metal and Metal Oxide Nanoparticles to Enhance the Performance of Enzyme-Linked Immunosorbent Assay (ELISA). *ACS Applied Nano Materials* 2020, 3, 1, 1-21.
14. Ciaurriz, P.; Fernández, F.; Tellechea, E.; Moran, J. F.; Asensio, A. C., Comparison of four functionalization methods of gold nanoparticles for enhancing the enzyme-linked immunosorbent assay (ELISA). *Beilstein journal of nanotechnology* **2017,** *8* (1), 244-253.

15. Vashist, S. K.; Dixit, C. K.; MacCraith, B. D.; O'Kennedy, R., Effect of antibody immobilization strategies on the analytical performance of a surface plasmon resonance-based immunoassay. *Analyst* **2011,** *136* (21), 4431-4436.
16. Vashist, S. K.; Luong, J. H., Antibody immobilization and surface functionalization chemistries for immunodiagnostics. In *Handbook of Immunoassay Technologies*, Elsevier: 2018; pp 19-46.
17. Zhou, H.-C.; Kitagawa, S., Metal-organic frameworks (MOFs). 2014,43, 5561-5593.
18. Niu, Z.; Gunatilleke, W. D. B.; Sun, Q.; Lan, P. C.; Perman, J.; Ma, J.-G.; Cheng, Y.; Aguila, B.; Ma, S., Metal-organic framework anchored with a Lewis pair as a new paradigm for catalysis. *Chem* **2018,** *4* (11), 2587-2599.
19. Li, H.; Wang, K.; Sun, Y.; Lollar, C. T.; Li, J.; Zhou, H.-C., Recent advances in gas storage and separation using metal–organic frameworks. *Materials Today* **2018,** *21* (2), 108-121.
20. Yi, F. Y.; Chen, D.; Wu, M. K.; Han, L.; Jiang, H. L., Chemical sensors based on metal–organic frameworks. *ChemPlusChem* **2016,** *81* (8), 675-690.
21. Stassen, I.; Burtch, N.; Talin, A.; Falcaro, P.; Allendorf, M.; Ameloot, R., An updated roadmap for the integration of metal–organic frameworks with electronic devices and chemical sensors. *Chemical Society Reviews* **2017,** *46* (11), 3185-3241.
22. Cui, Y.; Li, B.; He, H.; Zhou, W.; Chen, B.; Qian, G., Metal–organic frameworks as platforms for functional materials. *Accounts of chemical research* **2016,** *49* (3), 483-493.
23. Zhuang, J.; Young, A. P.; Tsung, C. K., Integration of biomolecules with metal–organic frameworks. *Small* **2017,** *13* (32), 1700880.
24. Liao, F.-S.; Lo, W.-S.; Hsu, Y.-S.; Wu, C.-C.; Wang, S.-C.; Shieh, F.-K.; Morabito, J. V.; Chou, L.-Y.; Wu, K. C.-W.; Tsung, C.-K., Shielding against unfolding by embedding enzymes in metal–organic frameworks via a de novo approach. *Journal of the American Chemical Society* **2017,** *139* (19), 6530-6533.
25. Wang, C.; Sun, H.; Luan, J.; Jiang, Q.; Tadepalli, S.; Morrissey, J. J.; Kharasch, E. D.; Singamaneni, S., Metal–organic framework encapsulation for biospecimen preservation. *Chemistry of Materials* **2018,** *30* (4), 1291-1300.
26. Doonan, C.; Ricco, R.; Liang, K.; Bradshaw, D.; Falcaro, P., Metal–organic frameworks at the biointerface: synthetic strategies and applications. *Accounts of chemical research* **2017,** *50* (6), 1423-1432.
27. Wang, C.; Sudlow, G.; Wang, Z.; Cao, S.; Jiang, Q.; Neiner, A.; Morrissey, J. J.; Kharasch, E. D.; Achilefu, S.; Singamaneni, S., Metal-Organic Framework Encapsulation Preserves the Bioactivity of Protein Therapeutics. *Advanced healthcare materials* **2018,** *7* (22), 1800950.
28. Li, S.; Liu, X.; Chai, H.; Huang, Y., Recent advances in the construction and analytical applications of metal-organic frameworks-based nanozymes. *TrAC Trends in Analytical Chemistry* **2018,** *105*, 391-403.
29. Li, J.; Cao, Y.; Hinman, S. S.; McKeating, K. S.; Guan, Y.; Hu, X.; Cheng, Q.; Yang, Z., Efficient label-free chemiluminescent immunosensor based on dual functional cupric oxide nanorods as peroxidase mimics. *Biosensors and Bioelectronics* **2018,** *100*, 304-311.
30. Wu, J.; Wang, X.; Wang, Q.; Lou, Z.; Li, S.; Zhu, Y.; Qin, L.; Wei, H., Nanomaterials with enzyme-like characteristics (nanozymes): next-generation artificial enzymes (II). *Chemical Society Reviews* **2019,** *48* (4), 1004-1076.

31. Ye, R.; Zhu, C.; Song, Y.; Lu, Q.; Ge, X.; Yang, X.; Zhu, M. J.; Du, D.; Li, H.; Lin, Y., Bioinspired synthesis of all-in-one organic–inorganic hybrid nanoflowers combined with a handheld pH meter for on-site detection of food pathogen. *Small* **2016,** *12* (23), 3094-3100.
32. Xu, N.; Bai, J.; Peng, Y.; Qie, Z.; Liu, Z.; Tang, H.; Liu, C.; Gao, Z.; Ning, B., Pretreatment-free detection of diazepam in beverages based on a thermometric biosensor. *Sensors and Actuators B: Chemical* **2017,** *241*, 504-512.
33. Mohammad, M.; Razmjou, A.; Liang, K.; Asadnia, M.; Chen, V., Metal–Organic-Framework-Based Enzymatic Microfluidic Biosensor via Surface Patterning and Biomineralization. *ACS applied materials & interfaces* **2018,** *11* (2), 1807-1820.
34. Lee, H.; Dellatore, S. M.; Miller, W. M.; Messersmith, P. B., Mussel-inspired surface chemistry for multifunctional coatings. *science* **2007,** *318* (5849), 426-430.
35. Tian, Y.; Cao, Y.; Wang, Y.; Yang, W.; Feng, J., Realizing ultrahigh modulus and high strength of macroscopic graphene oxide papers through crosslinking of mussel-inspired polymers. *Advanced materials* **2013,** *25* (21), 2980-2983.
36. Van Oss, C. J.; Chaudhury, M. K.; Good, R. J., Interfacial Lifshitz-van der Waals and polar interactions in macroscopic systems. *Chemical Reviews* **1988,** *88* (6), 927-941.
37. Vashist, S. K., Graphene-based immunoassay for human lipocalin-2. *Analytical biochemistry* **2014,** *446*, 96-101.
38. Zheng, D.; Vashist, S. K.; Al-Rubeaan, K.; Luong, J. H.; Sheu, F.-S., Mediatorless amperometric glucose biosensing using 3-aminopropyltriethoxysilane-functionalized graphene. *Talanta* **2012,** *99*, 22-28.
39. Liang, K.; Ricco, R.; Doherty, C. M.; Styles, M. J.; Bell, S.; Kirby, N.; Mudie, S.; Haylock, D.; Hill, A. J.; Doonan, C. J., Biomimetic mineralization of metal-organic frameworks as protective coatings for biomacromolecules. *Nature communications* **2015,** *6*, 7240.
40. Fotiadis, D.; Scheuring, S.; Müller, S. A.; Engel, A.; Müller, D. J., Imaging and manipulation of biological structures with the AFM. *Micron* **2002,** *33* (4), 385-397.
41. Beauchamp, J., Infrared Tables (short summary of common absorption frequencies). *Course Notes* **2010,** *2620*, 19.
42. Feng, Y.; Wang, H.; Zhang, S.; Zhao, Y.; Gao, J.; Zheng, Y.; Zhao, P.; Zhang, Z.; Zaworotko, M. J.; Cheng, P., Antibodies@ MOFs: An In Vitro Protective Coating for Preparation and Storage of Biopharmaceuticals. *Advanced Materials* **2019,** *31* (2), 1805148.
43. Wong-Ng, W.; Kaduk, J.; Espinal, L.; Suchomel, M.; Allen, A.; Wu, H., High-resolution synchrotron X-ray powder diffraction study of bis (2-methylimidazolyl)-zinc, C 8 H 10 N 4 Zn (ZIF-8). *Powder Diffraction* **2011,** *26* (3), 234-237.
44. Moazzam, P.; Tavassoli, H.; Razmjou, A.; Warkiani, M. E.; Asadnia, M., Mist harvesting using bioinspired polydopamine coating and microfabrication technology. *Desalination* **2018,** *429*, 111-118.
45. Noorisafa, F.; Razmjou, A.; Emami, N.; Low, Z.-X.; Korayem, A. H.; Kajani, A. A., Surface modification of polyurethane via creating a biocompatible superhydrophilic nanostructured layer: role of surface chemistry and structure. *Journal of Experimental Nanoscience* **2016,** *11* (14), 1087-1109.
46. Yang, H. C.; Waldman, R. Z.; Wu, M. B.; Hou, J.; Chen, L.; Darling, S. B.; Xu, Z. K., Dopamine: just the right medicine for membranes. *Advanced Functional Materials* **2018,** *28* (8), 1705327.

47. Liu, Q.; Wang, N.; Caro, J. r.; Huang, A., Bio-inspired polydopamine: a versatile and powerful platform for covalent synthesis of molecular sieve membranes. *Journal of the American Chemical Society* **2013,** *135* (47), 17679-17682.
48. Zhou, J.; Wang, P.; Wang, C.; Goh, Y. T.; Fang, Z.; Messersmith, P. B.; Duan, H., Versatile core–shell nanoparticle@ metal–organic framework nanohybrids: Exploiting mussel-inspired polydopamine for tailored structural integration. *ACS nano* **2015,** *9* (7), 6951-6960.
49. Wang, N.; Liu, Y.; Qiao, Z.; Diestel, L.; Zhou, J.; Huang, A.; Caro, J., Polydopamine-based synthesis of a zeolite imidazolate framework ZIF-100 membrane with high H 2/CO 2 selectivity. *Journal of Materials Chemistry A* **2015,** *3* (8), 4722-4728.
50. Tan, X.; Wang, X.; Zhang, L.; Liu, L.; Zheng, G.; Li, H.; Zhou, F., Stable and photothermally efficient antibody-covered Cu3 (PO4) 2@ polydopamine nanocomposites for sensitive and cost-effective immunoassays. *Analytical chemistry*. 2019, 91, 13, 8274-8279.
51. Zhang, H.; Chen, W.; Gong, K.; Chen, J., Nanoscale Zeolitic Imidazolate Framework-8 as Efficient Vehicles for Enhanced Delivery of CpG Oligodeoxynucleotides. *ACS applied materials & interfaces* **2017,** *9* (37), 31519-31525.
52. Wang, C.; Tadepalli, S.; Luan, J.; Liu, K. K.; Morrissey, J. J.; Kharasch, E. D.; Naik, R. R.; Singamaneni, S., Metal-Organic Framework as a Protective Coating for Biodiagnostic Chips. *Advanced Materials* **2017,** *29* (7), 1604433.
53. Liu, Y.; Wang, H.; Huang, J.; Yang, J.; Liu, B.; Yang, P., Microchip-based ELISA strategy for the detection of low-level disease biomarker in serum. *Analytica chimica acta* **2009,** *650* (1), 77-82.
54. Wang, C.; Gao, J.; Tan, H., Integrated antibody with catalytic metal–organic framework for colorimetric immunoassay. *ACS applied materials & interfaces* **2018,** *10* (30), 25113-25120.
55. Armbruster, D. A.; Pry, T., Limit of blank, limit of detection and limit of quantitation. *The clinical biochemist reviews* **2008,** *29* (Suppl 1), S49.
56. Liu, W.; Yang, H.; Ding, Y.; Ge, S.; Yu, J.; Yan, M.; Song, X., based colorimetric immunosensor for visual detection of carcinoembryonic antigen based on the high peroxidase-like catalytic performance of ZnFe 2 O 4–multiwalled carbon nanotubes. *Analyst* **2014,** *139* (1), 251-258.
57. Zhang, L.; Fan, C.; Liu, M.; Liu, F.; Bian, S.; Du, S.; Zhu, S.; Wang, H., Biominerized gold-Hemin@ MOF composites with peroxidase-like and gold catalysis activities: a high-throughput colorimetric immunoassay for alpha-fetoprotein in blood by ELISA and gold-catalytic silver staining. *Sensors and Actuators B: Chemical* **2018,** *266*, 543-552.
58. Gao, Z.; Lv, S.; Xu, M.; Tang, D., High-index {hk 0} faceted platinum concave nanocubes with enhanced peroxidase-like activity for an ultrasensitive colorimetric immunoassay of the human prostate-specific antigen. *Analyst* **2017,** *142* (6), 911-917.
59. Kim, W.-J.; Cho, H. Y.; Jeong, B.; Byun, S.; Huh, J.; Kim, Y. J., Synergistic Use of Gold Nanoparticles (AuNPs) and "Capillary Enzyme-Linked Immunosorbent Assay (ELISA)" for High Sensitivity and Fast Assays. *Sensors* **2018,** *18* (1), 55.
60. Petrakova, A.; Urusov, A.; Zherdev, A.; Dzantiev, B., Magnetic ELISA of aflatoxin B1–pre-concentration without elution. *Analytical Methods* **2015,** *7* (24), 10177-10184.
61. Eum, J. Y.; Hwang, S. Y.; Ju, Y.; Shim, J. M.; Piao, Y.; Lee, J.; Kim, H.-S.; Kim, J., A highly sensitive immunoassay using antibody-conjugated spherical mesoporous silica with immobilized enzymes. *Chemical Communications* **2014,** *50* (27), 3546-3548.

List of Figures

Figure 1. The workflow of the surface modification for the immunoassay using a PDA-PEI and ZIF-8 platform and their stability against high temperature and various pH. The microtitre ELISA plate coated with thin layer of PDA-PEI and the anti PD-L1 antibody was added in to precursors of ZIF-8, following the addition of the certain concentration of PD-L1 antigen and incubate for 1 hour in room temperature on 400 rpm plate shaker. The stability of proposed platform against elevating pH and temperature was also investigated during incubation time.

Figure 2. (A) SEM images of (I) antibody@ZIF-8/PDA-PEI, (II) ZIF-8/PDA-PEI, (III) PDA-PEI coated well, (IV) empty well with 5000x magnification (Scale bar: 2 μm). The thin film of PDA/PEI formed on the surface of microtiter ELISA wells. (B) AFM images of (I) empty well, (II) PDA-PEI coated well, (III)ZIF-8/PDA-PEI , (IV)antibody@ZIF-8/PDA-PEI. Surface roughness increases by formation of thin film of ZIF-8 on the surface of PDA-PEI coated wells.

Figure 3. (A) FT-IR spectra of antibody@ZIF-8/PDA-PEI, ZIF-8/PDA-PEI, PDA-PEI coated well and Empty well. Measurements were done from 4000 to 400 cm^{-1} and PDA-PEI showed intensive peak at 1650cm^{-1} whilst ZIF-8 have important peak at 426cm^{-1}. (B)XRD patterns of antibody@ZIF-8/ PDA-PEI, ZIF-8/PDA-PEI, PDA-PEI coated well and Empty well. The intensive peaks in 7.3, 10.3, 12.7, 16.5, 18 which is specific for ZIF-8 crystalline structure proves the dense formation of ZIF-8 crystalline layer on surface of microtitre ELISA plate. (C)Water Contact Angle and Surface Free Energy of antibody@ZIF-8/ PDA-PEI, ZIF-8/PDA-PEI, PDA-PEI coated well and Empty well.

Figure 4. ELISA for detection of PD-L1 antigen in exposure to various (A) temperatures and (B) pH and (C Standard Curve for PD-L1 antigen in PDA-PEI coated wells, antibody@ZIF-8 in PDA-PEI coated wells and empty wells. (D) The effect of decreasing antibody concentration on OD detection. Up to the concentration of 350pg/mL of PD-L1 antigen the detection graph was linear. The lines show linear trend line.

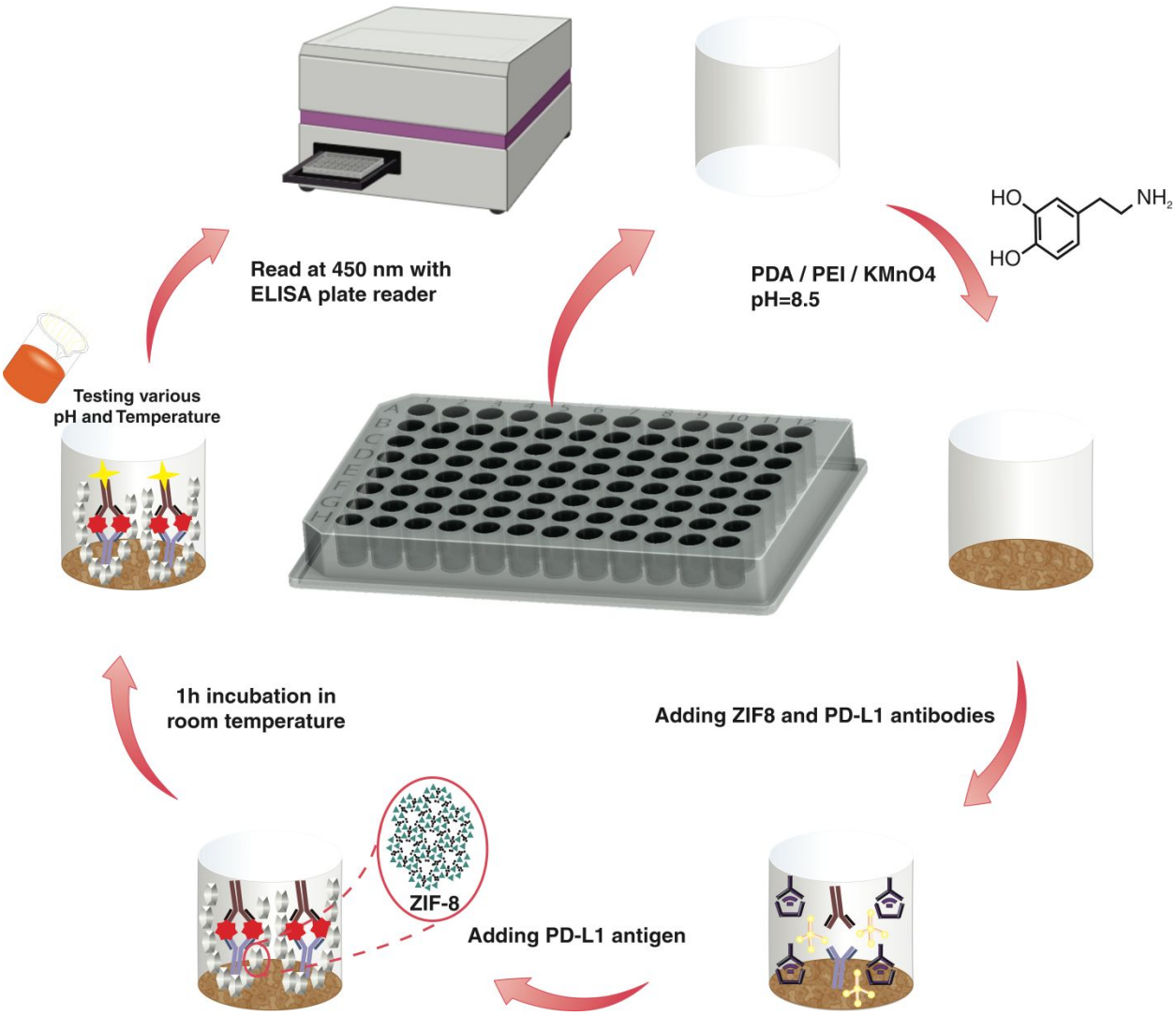
Read at 450 nm with
ELISA plate reader
PDA / PEI / KMnO4
pH=8.5
HO
HO
NH2
Testing various
pH and Temperature
1h incubation in
room temperature
Adding ZIF8 and PD-L1 antibodies
ZIF-8
Adding PD-L1 antigen

Figure 1

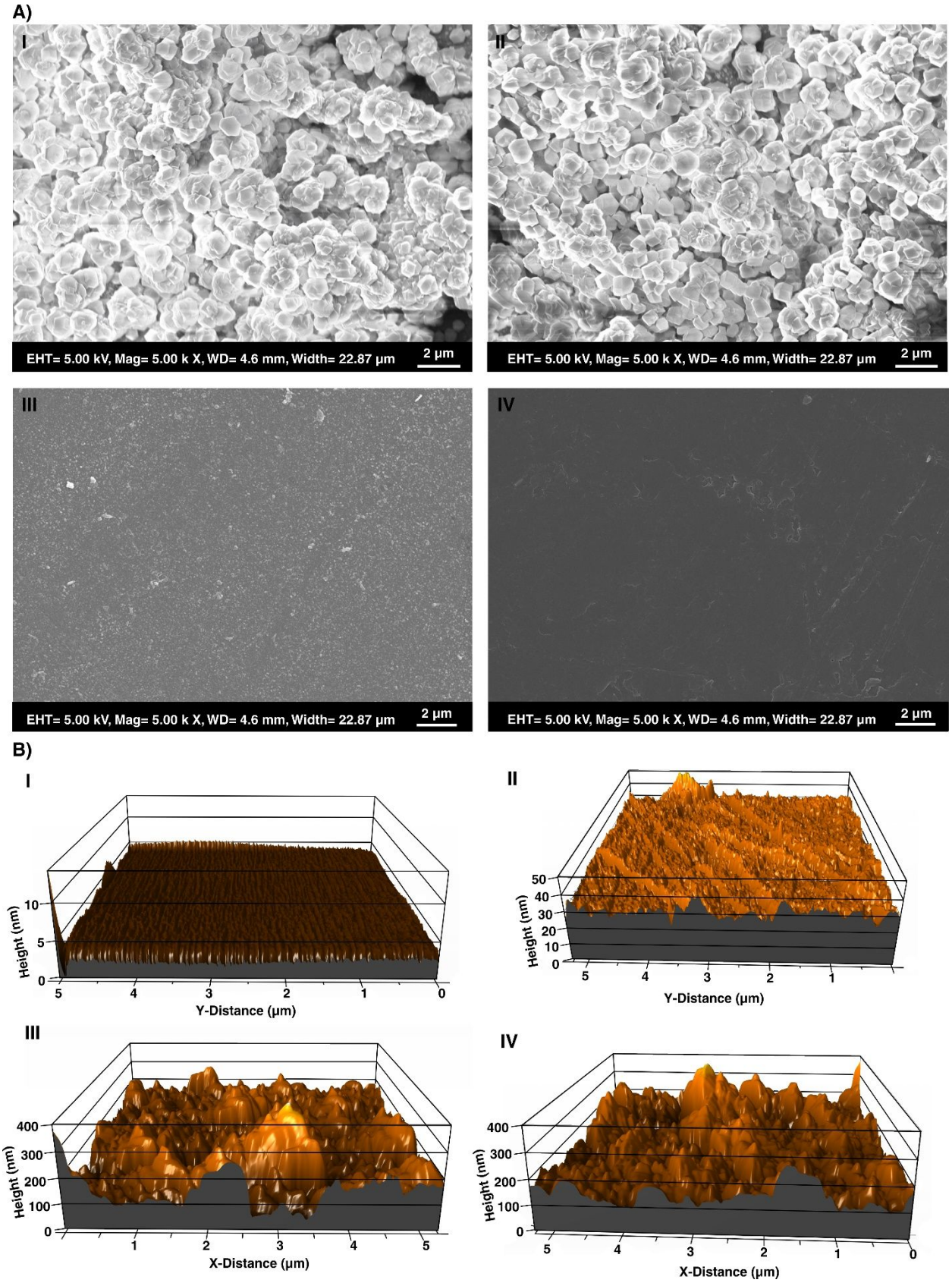
A)
I
EHT= 5.00 kV, Mag= 5.00 k X, WD= 4.6 mm, Width= 22.87 µm
2 µm
II
EHT= 5.00 kV, Mag= 5.00 k X, WD= 4.6 mm, Width= 22.87 µm
2 µm
III
EHT= 5.00 kV, Mag= 5.00 k X, WD= 4.6 mm, Width= 22.87 µm
2 µm
IV
EHT= 5.00 kV, Mag= 5.00 k X, WD= 4.6 mm, Width= 22.87 µm
2 µm
B)
I
Height (nm)
Y-Distance (µm)
II
Height (nm)
Y-Distance (µm)
III
Height (nm)
X-Distance (µm)
IV
Height (nm)
X-Distance (µm)

Figure 2

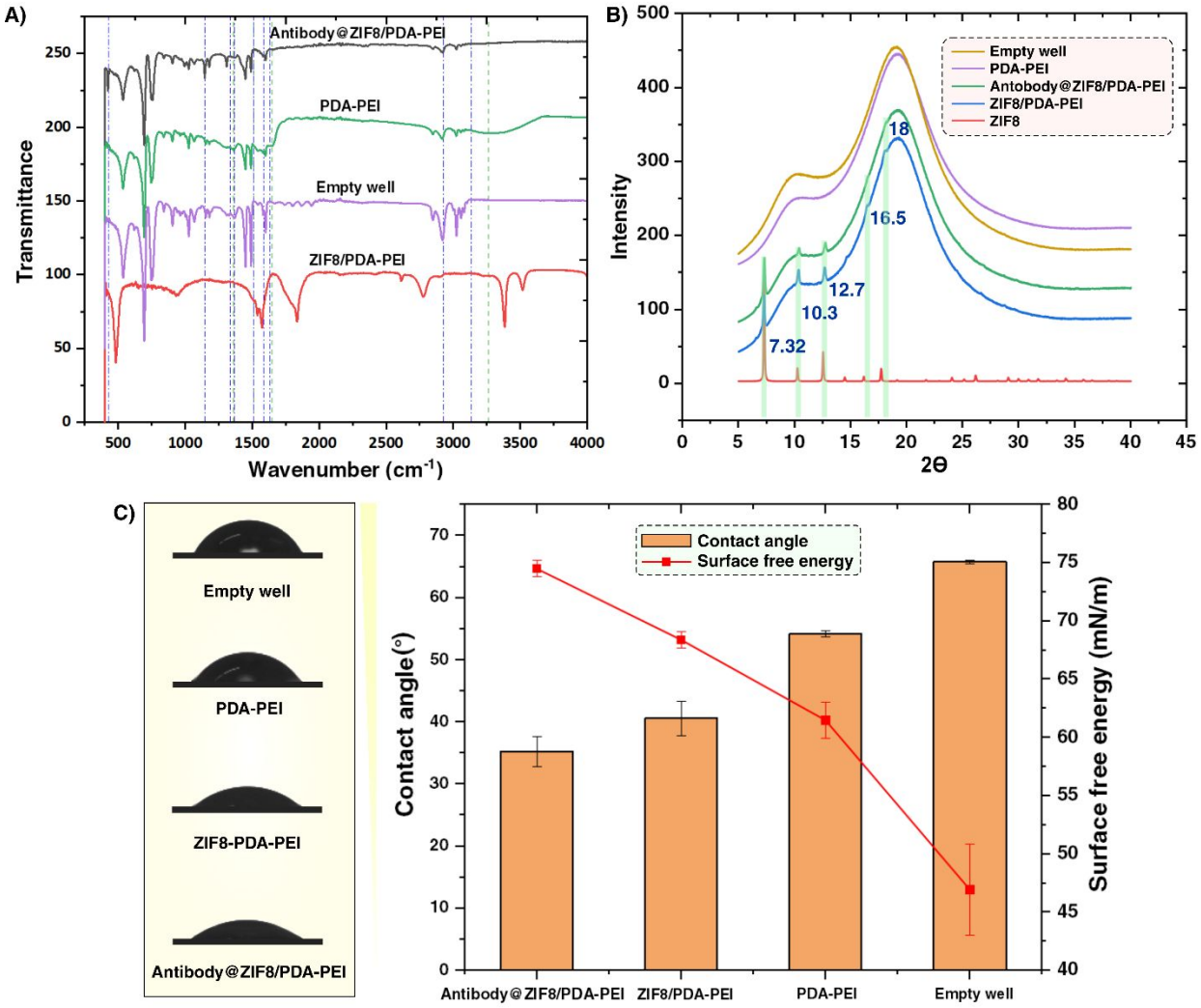
A)
Antibody@ZIF8/PDA-PEI
PDA-PEI
Empty well
ZIF8/PDA-PEI
Transmittance
Wavenumber (cm-1)
B)
Empty well
PDA-PEI
Antobody@ZIF8/PDA-PEI
ZIF8/PDA-PEI
ZIF8
Intensity
2Θ
18
16.5
12.7
10.3
7.32
C)
Empty well
PDA-PEI
ZIF8-PDA-PEI
Antibody@ZIF8/PDA-PEI
Contact angle
Surface free energy
Contact angle(°)
Surface free energy (mN/m)
Antibody@ZIF8/PDA-PEI
ZIF8/PDA-PEI
PDA-PEI
Empty well

Figure 3

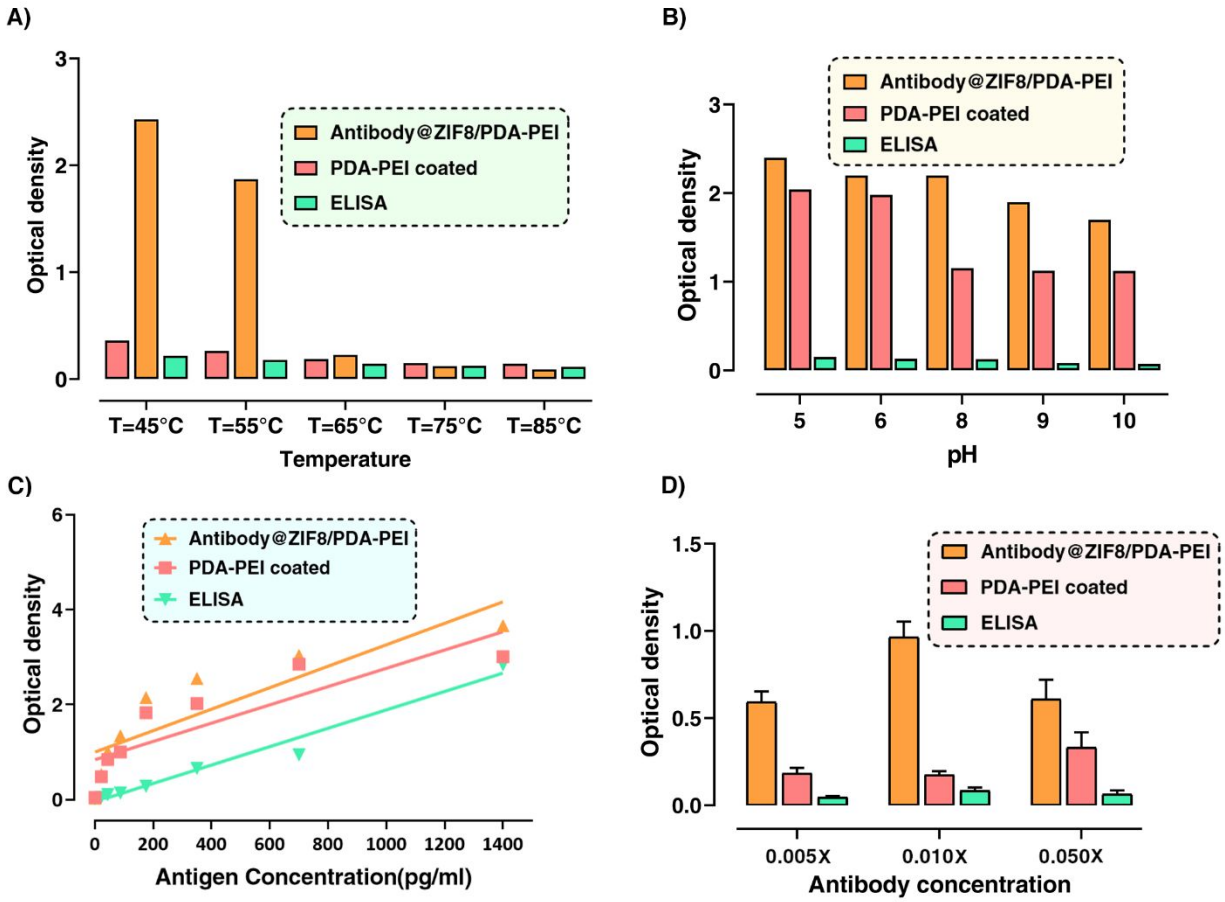
A)
Optical density
Antibody@ZIF8/PDA-PEI
PDA-PEI coated
ELISA
T=45°C
T=55°C
T=65°C
T=75°C
T=85°C
Temperature
B)
Optical density
Antibody@ZIF8/PDA-PEI
PDA-PEI coated
ELISA
pH
C)
Optical density
Antibody@ZIF8/PDA-PEI
PDA-PEI coated
ELISA
Antigen Concentration(pg/ml)
D)
Optical density
Antibody@ZIF8/PDA-PEI
PDA-PEI coated
ELISA
0.005X
0.010X
0.050X
Antibody concentration

Figure 4

Table 1. The comparison of using ZIF-8/PDA-PEI platform with other MOF, metal, and metal oxide-based platforms for ELISA in the literature.

Types of nanoparticles	**Signal**	**Analyte**	**Detection range**	**LOD**	**Comparison with traditional ELISA (LOD improvement)**	**Ref**
ZIF-8/PDA-PEI	Colorimetric	PD-L1	21.87 –1400 pg/mL	0.035 pg/mL	225-fold	This study
Platinum nanocubes	Colorimetric	Prostate-Specific Antigen	20-2000 pg/mL	0.8 pg/mL	10-fold	[58]
Gold nanoparticle	Colorimetric	C reactive protein	0.1 – 1000 ng/mL	0.1 ng/mL	100-fold	[59]
Magnetic nanoparticles	Colorimetric	Aflatoxin B1	0.002 – 0.2 ng/mL	2 pg/mL	10-fold	[60]
Mesoporous Silica nanoparticles Sandwich	Colorimetric	hIgG	0.1 – 1000 ng/mL	0.5 ng/mL	20-fold	[61]
ZnFe2O4@ multiwalled carbon nanotube	Colorimetric	Carcinoembryonic Antigen	0.005 – 30 ng/mL	2.6 pg/mL	77-fold	[56]
Hemin-Au@MOF	Colorimetric	alpha-fetoprotein	0.080 – 43 ng/mL	0.020 ng/mL	5-fold	[57]
Cu-MOF	Colorimetric	mIgG	1 – 100ng/mL	0.34 ng/mL	3-fold	[54]

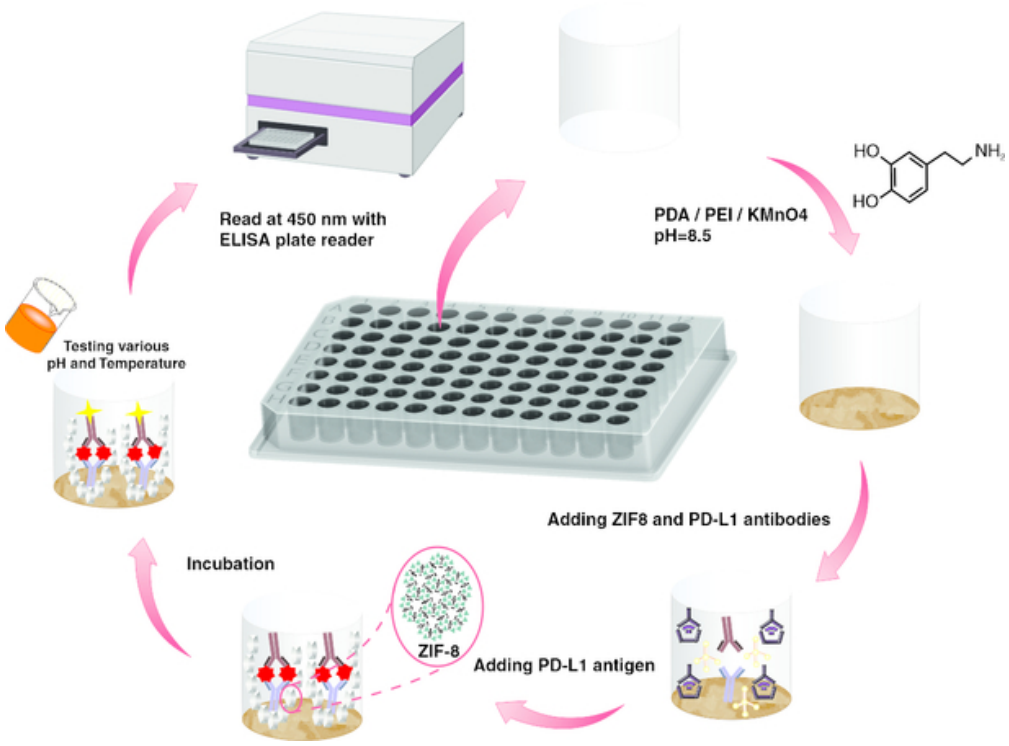

51x38mm (300 x 300 DPI)